Power flow model with flat frequency control and load characteristic for voltage stability indices

Power flow model with flat frequency control and load characteristic for voltage stability indices

Abraham Lomi[1], Awan Uji Krismanto[1], F Yudi Limpraptono[1], Kartiko Ardi Widodo[1], Ali Mahmudi[2], and Ahmad Faisol[2]

[1] Department of Electrical Engineering, National Institute of Technology, Malang, Indonesia
[2] Department of Informatics Engineering, National Institute of Technology, Malang, Indonesia

E-mail: abraham@lecturer.itn.ac.id

Abstract. The growing of power systems with massive interconnection becomes more complicated for reliable and economical operation under dynamic as well as steady-state operating conditions. Therefore, it is desirable to develop techniques for evaluating the voltage stability condition with the implementation of the voltage stability index and the minimum singular value of the system. This paper proposes an approach a model of power flow incorporating the generator controls with considering load characteristics of flat frequency control (FFC) scheme in large interconnected power systems. Results on a 24-Bus EHV practical system is presented for illustration of power flow solution.

1. Introduction

The load in a power system will change continually related to the variation of frequency and voltage system at the load buses and do not remain constant. It is necessary to consider a model with the load characteristics as a function of voltage and frequency, particularly when the voltage profile is forced to change with the application of the reactive power optimization in the system [1-3]. From the security of increasingly large and complex power systems, it is necessary to determine the frequency, voltage, and condition of a various component in the system during over and under load presence. Thus there is a need for a model which incorporates load, generation regulation and also tie-line control effects [4-5].

The power flow analysis in steady-state condition using the swing bus concept based on the conventional methods with the following assumptions:

- Frequency of the system remains constant.
- The load remains constant.
- All the generators except the swing bus generator remain constant.
- Only that swing bus generator meets the unbalanced power in the system.
- Assume the inter-connected bus and the tie-line are constant.

However, some of these assumptions may not be valid for practical power system operation.

System frequency, though can be maintained relatively constant during normal operating conditions, may change following a disturbance in the system such as loss of generation, load or tie-line support. It is not possible to represent tie-line control effect in the conventional load flow models without neglecting the steady-state frequency deviations and these models fail to provide a solution for a steady-state following a disturbance in the system

In this paper, a power flow model with flat frequency controls and load characteristic is presented for voltage stability index in large interconnected power systems. The proposed algorithm is to be suitable for the online application [6].

2. General approach

The approach is based on the de-coupling of active and reactive power optimization with the significant steps as follows:
Step A: Input of system data, loads, and constraints.
Step B: Active power optimization.
Step C: Security analysis for modification of the generating unit limits and branch flows.
Step D: Confirmation of satisfactory steady-state system performance.
Step E: Reactive power optimization.
Step F: Output results.
In the practical operation of power systems, Step A gives the details of a set of forecasted load conditions, generation costs, import/export details and costs, and network configuration/constraints, etc. Step B gives an optimal combination of active power dominated by economic objectives of minimizing active power generation costs. Step C does security analysis and provides corrective measures. In Step D, confirmation of satisfactory steady-state system performance is obtained. At this stage, a solution which has optimum active power generation and import/export schedule, besides satisfying the security constraints are obtained. Step E performs reactive power optimization using the active power generation schedule obtained in the earlier steps as the input. After getting the results of this step, again go through the steps C and D to obtain the final solution, where active and reactive power is optimally scheduled, and all the system performance constraints are met satisfactorily.

3. Generator model

The generator's prime mover responses as primary control and AGC actions as secondary controls are considered in this model. The active power generation at a bus *k* is defined as,

$$P_{Gk}^{act} = P_{Gk}^{sch} + P_{Gk}^{con} \tag{1}$$

$$P_{Gk}^{con} = -\frac{1}{r_k}.\Delta f + \alpha_k.\Delta G \tag{2}$$

$$\Delta G = \Delta P_T + B.\Delta f \tag{3}$$

where,

$$\sum \alpha_k = 1.00$$

$$\Delta f = f^{act} - f^{nom}$$

$$\Delta P_T = P_T^{act} - P_T^{nom}$$

$$P_{Gk}^{\min} \le P_{Gk}^{act} \le P_{Gk}^{\max}$$

Δf : the system steady-state frequency deviation; ΔG : the error of static area control; r is the turbine governor speed droop setting in the generating plant at a bus; α : the generator participation factor in the secondary control of a bus; B : the bias factor setting of an AGC regulator; P_T is the tie-line exchange power.
Flat frequency control is one the possible way of automatic generation controls to be considered.

4. Load model

The load's power is modelled as a function of the voltage at the bus and the system frequency steady-state deviation. The active and reactive power loads at bus *k* are considered as follows:

$$P_{Lk}^{act} = P_{Lk}^{sch}(1 + f_{1k}\Delta f)(A_{1k} + A_{2k}.V_k + A_{3k}V_k^2 + A_{4k}V_k^{ep}) \tag{4}$$

$$Q_{Lk}^{act} = Q_{Lk}^{sch}(1 + f_{2k}\Delta f)(R_{1k} + R_{2k}.V_k + R_{3k}V_k^2 + R_{4k}V_k^{eq}) \tag{5}$$

Where f_1 and f_2 are coefficients of frequency dependence of active and reactive load. A_1, A_2, A_3, A_4 and R_1, R_2, R_3, R_4 are coefficients of the active load proportional to constant power, constant current, constant impedance, *ep*th power of voltage at the bus and reactive load proportional to constant power, constant current, constant impedance, *eq*th power of voltage at the bus, respectively.

5. Classification of buses and variables

If the number of total buses and generators in a system are represented by n and g respectively, it is assumed that,

1, 2, ..., g is the generator buses, and

g+1, g+2, ..., n are the remaining buses.

Buses 1, 2, ..., g are with regulating plants, and variable active power injections comprise the regulating power plants participating in primary and secondary system control and also regulated the voltage buses. The change of reactive power injection performs voltage regulation. Unknown variables related to these buses are,

- injected active powers (P_{Gk}^{act} , $k = 1, \ldots, g$)
- injected reactive powers (Q_{Gk}^{act} , $k = 1, \ldots, g$)
- the phase angle of voltages (δ_k , $k = 2, \ldots, g$)

Buses g+1, …, n are un-regulating plants, since there is no connection between plants and buses. The unknown variables related to these buses are,

- bus voltage magnitudes (V_k , $k = g+1, \ldots, n$)
- the phase angle of voltages (δ_k , $k = g+1, \ldots, n$)
- active power loads (P_{Lk}^{act} , $k = g+1, \ldots, n$)
- reactive power loads (Q_{Lk}^{act} , $k = g+1, \ldots, n$)

For assigned active and reactive loads given as steady-state frequency deviation and bus voltages of known functions. Apart from these variables, ΔG and Δf are also unknown. But these two variables do not appear as unknowns simultaneously. Either of them is unknown depending upon the AGC control strategies.

With the assumption of bus 1 as the reference for the voltage phase angle calculations with $\delta_1 = 0.0$, and $X = \Delta f$ or ΔG, the total number of unknowns is n, viz.,

$$X\ ,\ \delta_2\ , \ldots,\ \delta_g\ ,\ \delta_{g+1}, \ldots,\ \delta_n\ ,\ V_{g+1}, \ldots,\ V_n$$

6. Solution techniques

Separating the active and reactive part of the complex power balance in the system, $2n$ number of non-linear equations can be obtained. These equations at a node k are given by,

$$P_k^{net} = \sum_{m=1}^{n} V_k V_m Y_{km} \cos(\delta_k - \delta_m - \theta_{km}) \tag{6}$$

$$Q_k^{net} = \sum_{m=1}^{n} V_k V_m Y_{km} \sin(\delta_k - \delta_m - \theta_{km}) \tag{7}$$

$$P_{generation}^{act} - P_{load}^{act} = P^{net}$$

$$(P_{Gk}^{sch} + P_{Gk}^{con}) - P_{Lk}^{act} = P_k^{net}$$

or,

$$P_{Gk}^{sch} = -P_{Gk}^{con} + P_{Lk}^{act} + P_k^{net} \tag{8}$$

$$Q_{generation}^{act} - Q_{load}^{act} = Q^{net}$$

$$Q_{Gk}^{act} - Q_{Lk}^{act} = Q_k^{net}$$

or,

$$Q_{Gk}^{act} = Q_{Lk}^{act} + Q_k^{net} \tag{9}$$

The set of equations are obtained from the equations (8) and (9) for the application of Newton-Raphson iterative technique to get the unknown quantities. It is important to consider the fact that the active power injected at a bus does not change for a small change in the phase angle of the bus voltage. The effect of corresponding sensitivity coefficients and frequency deviation on reactive loads are negligible and therefore generally $F_2 = 0$ in equation (5), and if so, the linearized model can be solved by the Newton-Raphson iterative solution and can be written as,

$$\begin{bmatrix} \Delta P_1 \\ \Delta P_2 \\ \cdots \\ \Delta P_n \end{bmatrix} = \begin{bmatrix} \frac{\partial P_1}{\partial X} & \frac{\partial P_1}{\partial \delta_2} & \cdots & \frac{\partial P_1}{\partial \delta_n} \\ \frac{\partial P_2}{\partial X} & \frac{\partial P_2}{\partial \delta_2} & \cdots & \frac{\partial P_2}{\partial \delta_n} \\ \cdots & \cdots & \cdots & \cdots \\ \frac{\partial P_n}{\partial X} & \frac{\partial P_n}{\partial \delta_2} & \cdots & \frac{\partial P_n}{\partial \delta_n} \end{bmatrix} \begin{bmatrix} \Delta X \\ \Delta \delta_2 \\ \cdots \\ \Delta \delta_n \end{bmatrix} \tag{10}$$

and

$$\begin{bmatrix} \Delta Q_{g+1} \\ \Delta Q_{g+2} \\ \cdots \\ \Delta Q_n \end{bmatrix} = \begin{bmatrix} \frac{\partial Q_{g+1}}{\partial V_{g+1}} & \frac{\partial Q_{g+1}}{\partial V_{g+2}} & \cdots & \frac{\partial Q_{g+1}}{\partial V_n} \\ \frac{\partial Q_{g+2}}{\partial V_{g+1}} & \frac{\partial Q_{g+2}}{\partial V_{g+2}} & \cdots & \frac{\partial Q_{g+2}}{\partial V_n} \\ \cdots & \cdots & \cdots & \cdots \\ \frac{\partial Q_n}{\partial V_{g+1}} & \frac{\partial Q_n}{\partial V_{g+2}} & \cdots & \frac{\partial Q_n}{\partial V_n} \end{bmatrix} \begin{bmatrix} \Delta V_{g+1} \\ \Delta V_{g+2} \\ \cdots \\ \Delta V_n \end{bmatrix} \tag{11}$$

where,

$$\frac{\partial P_k}{\partial X} = -\left(-\frac{1}{r_k} + \alpha_k\right) + P_{Lk}^{sch}(f_{1k})(A_{1k} + A_{2k}V_k + A_{3k}V_k^2 + A_4 V_k^{ep})$$

$$\frac{\partial P_k}{\partial \delta_k} = -Q_k - B_{kk}V_k^2$$

$$\frac{\partial P_k}{\partial \delta_m} = V_k V_m Y_{km} \cos(\delta_k - \delta_m - \theta_{km})$$

$$\frac{\partial Q_k}{\partial V_k} = \frac{Q_k}{V_k} + B_{kk}V_k + Q_{Lk}^{sch}(R_{2k}V_k + 2R_{3k}V_k + R_4.eq.V_k^{eq-1})$$

$$\frac{\partial Q_k}{\partial V_m} = V_k V_m Y_{km} \sin(\delta_k - \delta_m - \theta_{km})$$

The relation (10) and (11) can be rewritten in a compact form as,

$$[\Delta P] = [J_1]\begin{bmatrix} \Delta X \\ \Delta \delta \end{bmatrix} \tag{12}$$

$$[\Delta Q] = [J_2][\Delta V] \tag{13}$$

where $X = \Delta G$ or Δf

The changes in power are the differences between the specified and calculated values as,

$$P^{(i)} = P_{specified} - P_{calculated}$$

$$Q^{(i)} = Q_{specified} - Q_{calculated}$$

where (i) is the iteration count. To evaluate the element of the Jacobian matrices [J_1] and [J_2], the estimated bus voltage, X, and the calculated powers are used. The triangular matrix factor of the

Jacobian matrices are used to solve parameters ΔX, $\Delta\delta$ and ΔV from the equations (12) and (13). The new estimates for the unknown, are

$$X^{(i+1)} = X^{(i)} + \Delta X^{(i)}$$
$$\delta^{(i+1)} = \delta^{(i)} + \Delta\delta^{(i)}$$
$$V^{(i+1)} = V^{(i)} + \Delta V^{(i)}$$

The process of iterative is repeated until $\Delta P^{(i)}$ and $\Delta Q^{(i)}$ for all the buses are within a specified tolerance.

7. Computational procedures

The computational steps to optimize the reactive power allocation in an interconnected power system is described in figure 1 as follows [7].

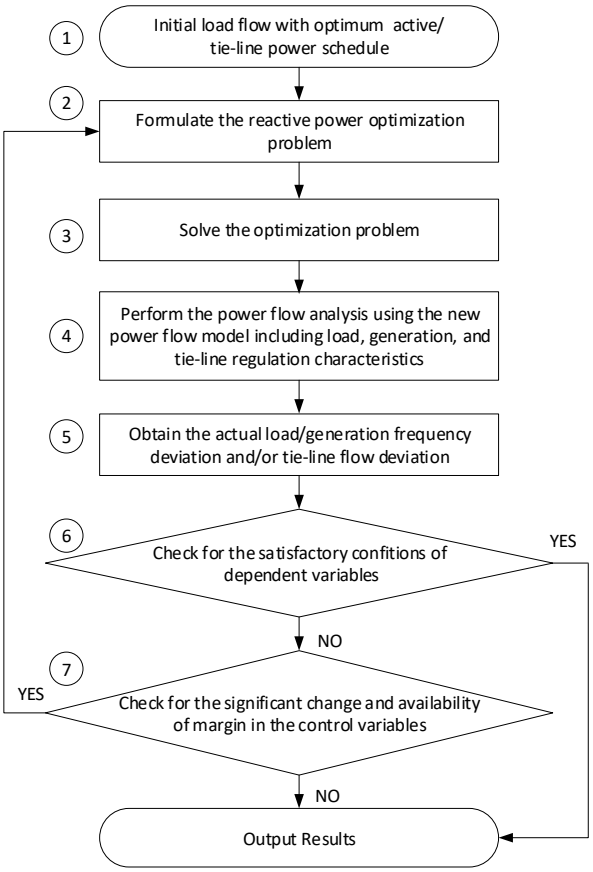

Figure 1. Flow chart of the algorithm for reactive power optimization in Large Inter-connected Power systems.

The scheme of the proposed algorithm for reactive power optimization in figure 1 is described as follows. Block-1 performs the load flow using a conventional power flow method for a given load condition with active power generation, tie-line flow schedule as obtained from an active power optimization technique [8]. This will be the initial condition for starting the reactive power optimization routine. Block-2 formulates the reactive power optimization problem, as explained in the following sections. Block-3 obtains the optimum settings using linear programming technique for the reactive power control variables [9], [10]. Block-4 evaluates the steady-state behaviour of the system using the power flow model described in this paper. When the settings of the reactive power control

variables are varied, the voltage profile in the system varies, which leads to a change in load conditions. To meet the new load demand generation schedule has also to be changed accordingly. If the active power generation is not matched correctly, the system steady-state frequency deviates from the nominal value. As the load and generation characteristics are included in the present model, besides representing the tie-line control effects, the actual steady state behavior of the system can, therefore, be easily analysed. Block-5 gives the actual picture of load/generation conditions in the system as well as tie-line flows. In addition, the static area control error consisting to the steady-state frequency deviation and/or tie-line flow deviations and compute depending upon the tie-line control strategies, i.e., Flat frequency control (FFC), Flat tie-line control (FTC), and Flat tie-line bias control (TBC) [7], [11]. Block-6, checks for the acceptable limits of the dependent variables. Computation from Block-2 through Block-6 form one iteration of VAR control process. Block-7 checks for the availability of margins on the control variables and significant change in the control of satisfactory conditions for the dependent variables. This iterative process is terminated when adequate conditions for the dependent variable are realized, or all the reactive power sources are exhausted. Block-7 provides the final information regarding the optimum settings for all the reactive power control variables, actual load, and generation conditions, tie-line flows, and the system frequency deviation and tie-line exchange deviations. This result is confirmed by going through security analysis. The final result will help the system operator to suitably modify the active and reactive power schedules for optimum operation of the system, besides satisfying the operating constraints.

8. System test case and case results

In this paper, a sample power flow study results are presented with flat-frequency control strategy option, while the generation control is not considered. The developed algorithm has been tested and simulated on a 24-Bus EHV test system with fixed load, and load characteristics are presented for illustration purposes. However, it is important to consider the effects of *QV*-control in reactive power dispatch problem [6-7]. Thus the load characteristics are considered with the defined coefficients taken as,

$A_1 = 1.0$; $A_2 = 0.0$; $A_3 = 0.0$; $A_4 = 0.0$;
$R_1 = 0.2$; $R_2 = 0.3$; $R_3 = 0.5$; $R_4 = 0.0$;
$f_1 = 0.0$ $f_2 = 0.0$

Results for power flow and static voltage stability indices are obtained for two cases:

- Without load characteristics
- With load characteristics

The system load is uniformly increased until the power flow shows a diverging tendency, and voltage stability indeces are observed. Results for the typical load conditions are presented. The data of the system (network and load data) are given in [12].

8.1. 24-Bus EHV System without Load Characteristics

The system data is given in [12]. The single line diagram of 24-Bus EHV system is shown in figure 2. The voltage profile and voltage stability index values obtained from the power flow method described are shown in figure 3 and figure 4, respectively. The summary results of the system are given in table 1.

Table 1. Summary results of 24-Bus test system without load characteristics

	Without load characteristics					
	Base case		Load increased 5%		Load increased 10%	
	MW	MVAR	MW	MVAR	MW	MVAR
Total Generation	2684.90	1046.30	2830.60	1329.20	3026.30	2108.10
Total P-Q Load	2620.00	980.00	2751.00	1029.00	2882.00	1078.00

Total Power Loss	64.94	-986.14	79.49	-707.50	119.40	344.94
Percentage Loss	2.42%		2.81%		4.77%	
$\boldsymbol{V_{min}}$	$V_{13} = 0.847$		$V_{13} = 0.812$		$V_{13} = 0.587$	
$\boldsymbol{V_{max}}$	$V_{1\text{-}4} = 1.000$		$V_{1\text{-}4} = 1.000$		$V_{1\text{-}2} = 1.000$	
$\boldsymbol{L_{max}}$	$L_8 = 0.54$		$L_8 = 0.62$		$L_{13} = 1.02$	
$\sum \boldsymbol{L^2}$	2.551		3.192		7.887	
MSV	0.78		0.69		0.00 (nearly)	

As can be seen from the results in table 1, the overall voltage stability index (ΣL^2) in the case without load characteristics of the system is increased from 2.551 (base case) to 3.192 where the load increased up to 5% and 7.887 where load increased up to 10%. Some of the load bus *L*-indices have reached 1.0, indicating that the system enters an unstable condition. This can also be observed from the voltages profile, which indicates the worst voltage profile of 0.587 p.u at bus number 13.

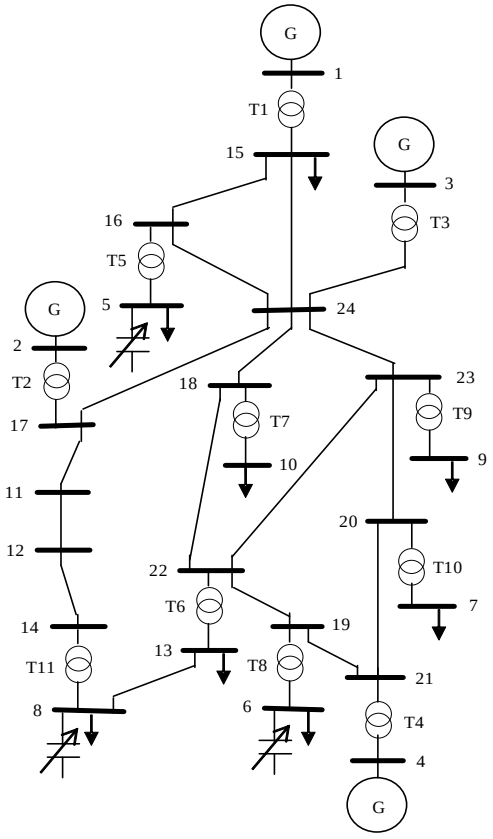

Figure 2. Single line diagram of 24-Bus EHV Test System.

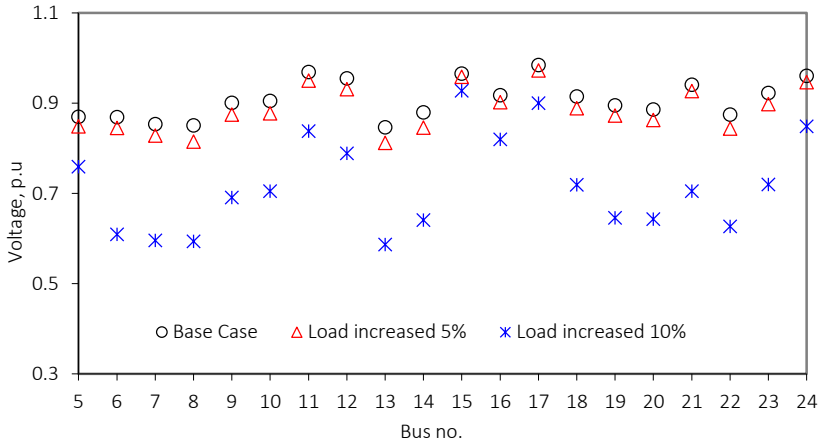

Figure 3. System voltage profiles without load characteristics.

Even from figure 3, we can observe that there are two nodes (bus nos. 8 and 13) where *L*-index values are beyond 1.0 (unstable). The minimum singular value of the system is decreased from 0.78 to 0.00 (nearly), indicating voltage instability.

8.2. 24-Bus EHV system with load characteristics

In this case, the system is considered with load characteristics. There are two levels of increased load conditions of the base case studied to observe voltage profile and voltage stability indices of the system. From the base case, the load is increased to 5%, and 10%. This is to show how far we can increase the load by observing the voltage stability index value. The voltage and voltage stability index value of the system at different load levels obtained from the load flow results are plotted. The voltage profiles and voltage stability indices at various load levels are shown in figure 4 and figure 5.

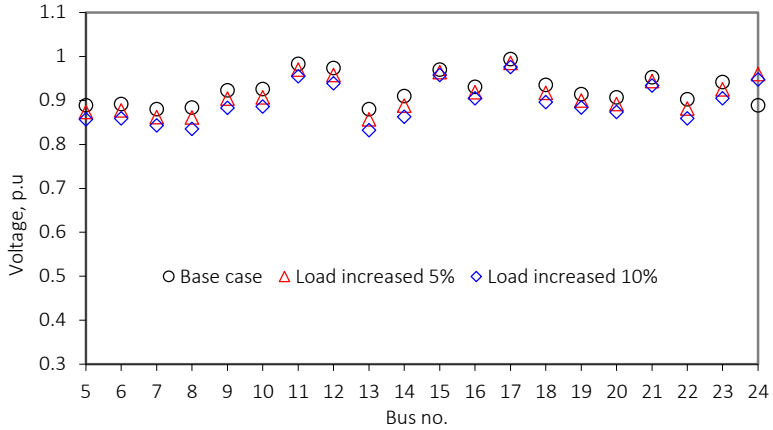

Figure 4. System voltage profiles with load characteristics.

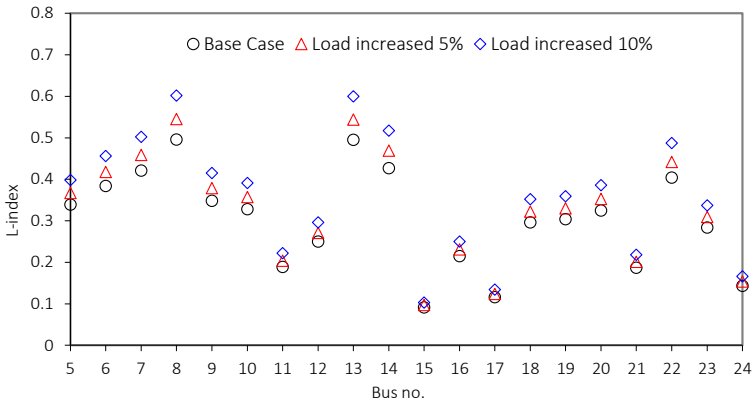

Figure 5. System voltage stability index with load characteristics.

The summary results of the system with load characteristics are given in table 2. Table 3 shows the system condition with and without load characteristics. When the load increases to 10% of the base case, the system enters to an unstable state. This is indicated by observing the voltage stability index value of 2 buses, i.e., 1.017 for bus 8 and 1.019 for bus 13 respectively.

Table 2. Summary results of 24-Bus EHV test system with load characteristics

	With load characteristics					
	Base case		Load increased 5%		Load increased 10%	
	MW	MVAR	MW	MVAR	MW	MVAR
Total Generation	2681.05	854.59	2823.83	1066.10	2969.08	1309.63
Total P-Q Load	2620.00	873.60	2751.00	899.06	2882.00	921.56
Total Power Loss	60.95	-1108.62	72.78	-891.6.50	87.03	-634.13
Percentage Losses	2.28%		2.58%		2.93%	
$\boldsymbol{V_{min}}$	V_{13} = 0.880		V_{13} = 0.857		V_{13} = 0.832	
$\boldsymbol{V_{max}}$	$V_{1\text{-}4}$ = 1.000		$V_{1\text{-}4}$ = 1.000		$V_{1\text{-}4}$ = 1.000	
$\boldsymbol{L_{max}}$	L_8 = 0.496		L_8 = 0.545		L_8 = 0.602	
$\boldsymbol{\sum L^2}$	2.208		2.624		3.148	
MSV	0.86		0.81		0.73	

Table 2 gives the static voltage stability indicators at various load level conditions. When the load increases to 10%, the system remains stable. This is indicated by the *L*-indices value. It is seen from figure 5 that the overall voltage stability *L*-indices (ΣL^2) are increased from 2.208, 2.624, and 3.148 when the load increased by 5% and 10%, respectively. This can also be observed from the voltage profiles shown in figure 4, which indicates the lower voltage profile of about 0.843 p.u and 0.832 p.u at buses 7 and 13 respectively.

Table 3. Summary results of 24-Bus EHV system with and without load characteristics: Base case

	Without load characteristics		With load characteristics	
	MW	MVAR	MW	MVAR
Total Generation	2684.98	1046.30	2681.05	854.59
Total P-Q Load	2620.00	980.00	2620.00	837.62
Total Power Loss	69.94	-986.14	60.95	-1108.60

Percentage Losses	2.42%	-	2.28%	-

The minimum singular value of the system is decreased from 0.86 to 0.73, indicating voltage remains stable. It can be seen from the results in Table 3 that the total generation in reactive power decrease from 1046.30 MVAR (without load characteristics) to 854.59 MVAR (with load characteristics), a reduction of about 18% and the total Q load is reduced from 980 MVAR to 837.62 MVAR, a decrease of about 14.5%. While the system P-load is same in both the cases, however, the total real power losses are more 64.94 MW (without load characteristics) and less 60.95 MW (with load characteristics).

9. Conclusion

A more realistic power flow model incorporating generation control and load characteristic is presented. A computationally, efficient approach is presented to obtain static voltage stability indices. The power flow model provides a practical steady-state solution for large interconnected systems during normal operating conditions and also during abnormal conditions following a disturbance. Static voltage stability analyses are carried out on typical systems. The results presented illustrate the effect of load characteristics which is important to consider in voltage stability analysis. It also indicates the severity of critical nodes vulnerable to voltage instability.

10. References

[1] Thukaram D, Parthasarathy K, Khincha HP, and Ramakrishna Iyengar BS, 1984 Steady-state Power Flow Analysis Incorporating Load and Generation Characteristics, *Journal of the Institution of Engineers* (I), Vol. **64**, pp. 274-279.

[2] Qiu J and Shahidehpour S M 1987 A New Approach for Minimization Power Loss and Improving Voltage Profile, *IEEE Trans. On Power Systems*, Vol.PWRS-**2**, No.2, pp. 287-296.

[3] Overbye T J 1994 Effects of Load Modelling on Analysis of Power System Voltage Stability, *Electric Power & Energy Systems*, Vol. 16, No.5, pp.329-338.

[4] Yao, Mengqi, Daniel K Molzahn, and Johanna L Mathieu 2019 An Optimal Power Flow Approach to Improve Power System Voltage Stability Using Demand Response, *IEEE Transactions on Control of Network Systems*, pp. 1-10.

[5] Lomi A and Limpraptono F Y 2018 Optimum allocation of reactive power sources for voltage stability improvement and loss minimization in power distribution system, *International Journal of Telecommunication, Electronic, and Computer Engineering*, Vol. **10**, No. 2-3, pp. 9-13.

[6] Bansilal, Thukaram D, and Parthasarathy K 1996 Optimal Reactive Power Dispatch Algorithm for Voltage Stability Improvement, *Electric Power Systems*, Vol.**18**, No.7, pp. 461-468.

[7] Lomi A, and Thukaram D 2012 Reactive Power Dispatch or Alleviation of Voltage Deviations, *TELKOMNIKA Jurnal*, Vol. **10**, No. 2, pp. 257-264.

[8] Mamandur K R C and Chenoweth R O 1981 Optimal Control of Reactive Power Flow for Improvements in Voltage Profiles and Real Power Minimization, *IEEE Trans. On PAS*. Vol.PAS-**100**, pp. 3185-3194.

[9] Deeb N and Shahidehpour S M 1988 An Efficient Technique for Reactive Power Dispatch Using a Revised Linear Programming Approach, *Electric Power Systems Research Journal*, Vol.**15**, pp.121-134.

[10] Alsac O, Bright J, Paris M and Stott B 1990 Further Developments in LP-Based Optimal Power Flow, *IEEE Trans. On Power Systems*, Vol. **5**, No.3, pp.697-711.

[11] Thukaram, D and Lomi A 2000 Selection of Static VAR Compensator Location and Size for System Voltage Stability Improvement, *The International Journal of Electric Power System Research*, **54**, pp. 139-150.

[12] Lomi A 2000 Planning and Operation of Reactive Power Sources for Voltage Stability Improvement and Harmonics Minimization, *Dissertation*, AIT Thailand.

Acknowledgments

The Authors wishing to thank you Directorate of Research and Community Service Ministry of Research, Technology, and Higher Education for supporting this research work for fiscal year 2019, under the contract No. 7/E/KPT/2019.

- **The below form will not be published, but it will help us to understand your paper better**

Authors' background

Name	**Email**	**Position** (Prof , Assoc. Prof. etc.)	**Research Field**	**Homepage URL**
Abraham Lomi	abraham@lecturer.itn.ac.id	Professor	Power System Stability, Power Electronics, Power Quality, Renewable Energy, Smart Grid	http://ee.itn.ac.id/abraham
Awan Uji Krismanto	awan_uji_krismanto@lecturer.itn.ac.id	Asistant Prof	Power System Stability, Smart Grid	
F Yudi Limpraptono	fyudil@lecturer.itn.ac.id	Assoc. Prof	Embedded System, Computer Network	
Kartiko Ardi Wibowo	kartikoardiw@gmail.com	Asistant Prof	Telecommunication system	
Ali Mahmudi	alimahmudi@gmail.com	Asistant Prof	Electronics	
Ahmad Faisol	mzfais@lecturer.itn.ac.id	Asistant Prof	Computer Science	